International Journal of Applied Earth Observation and Geoinformation 33 (2014) 312–320

Contents lists available at ScienceDirect

International Journal of Applied Earth Observation and Geoinformation

journal homepage: www.elsevier.com/locate/jag

Temporal disparity in leaf chlorophyll content and leaf area index across a growing season in a temperate deciduous forest

H. Croft[a,*], J.M. Chen[a], Y. Zhang[b]

[a] University of Toronto, Department of Geography, Toronto M5S 3G3, Canada
[b] Division of Biological and Physical Sciences, Delta State University, Cleveland, MS 38733, USA

ARTICLE INFO

Article history:
Received 7 May 2014
Accepted 12 June 2014
Available online 16 July 2014

Keywords:
Remote sensing
Phenology
GPP
Leaf physiology
Canopy structure

ABSTRACT

Spatial and temporal variations in canopy structure and leaf biochemistry have considerable influence on fluxes of CO_2, water and energy and nutrient cycling in vegetation. Two vegetation indices (VI), NDVI and Macc01, were used to model the spatio-temporal variability of broadleaf chlorophyll content and leaf area index (LAI) across a growing season. Ground data including LAI, hyperspectral leaf reflectance factors (400–2500 nm) and leaf chlorophyll content were measured across the growing season and satellite-derived canopy reflectance data was acquired for 33 dates at 1200 m spatial resolution. Key phenological information was extracted using the TIMESAT software. Results showed that LAI and chlorophyll start of season (SOS) dates were at day of year (DOY) 130 and 157 respectively, and total season duration varied by 57 days. The spatial variability of chlorophyll and LAI phenology was also analyzed at the landscape scale to investigate phenological patterns over a larger spatial extent. Whilst a degree of spatial variability existed, results showed that chlorophyll SOS lagged approximately 20–35 days behind LAI SOS, and the end of season (EOS) LAI dates were predominantly between 20 and 30 days later than chlorophyll EOS. The large temporal differences between VI-derived chlorophyll content and LAI has important implications for biogeochemical models using NDVI or LAI to represent the fraction of photosynthetically active radiation absorbed by a canopy, in neglecting to account for delays in chlorophyll production and thus photosynthetic capacity.

Introduction

Spatiotemporal variation in ecosystem properties such as canopy structure and leaf biochemistry has profound impacts on CO_2, water and energy fluxes and nutrient cycling (Churkina et al., 2005; Richardson et al., 2009b; Zhang et al., 2006). Leaf biochemistry is an important indicator of forest health, vegetation stress through disease or drought (Carter and Knapp, 2001) and is crucial to monitoring vegetation response to climate change (Morin et al., 2009) and for the inclusion within climate and ecological models (Morisette et al., 2009). Leaf area index (LAI), defined as one half the total (all-sided) green leaf area per unit ground surface area (Chen and Black, 1992), exhibits a major control on transpiration, CO_2 uptake and the interception of light and water by the canopy (Boegh et al., 2002; Houborg and Boegh, 2008). Ecological systems are highly complex and dynamic, with temporal variations in vegetation phenology and biophysical variables being far from uniform across space, both within and between species (Richardson et al., 2006, 2009a). However, many ecological studies use satellite-derived products to approximate vegetation 'greenness', as a composite of vegetation composition, structure and function (Pfeifer et al., 2012). Whilst this amalgam of canopy physical and biochemical properties implicitly assumes a correlation in time and space, research has shown that in addition to LAI, leaf structure and chemistry also vary across a growing season (Demarez et al., 1999; Kodani et al., 2002). Consequently, temporal and spatial variations in reflectance factors can be attributed to variations in vegetation properties at both canopy-level (LAI) and leaf-level (chlorophyll) (Croft et al., 2013; Zhang et al., 2006). Differences in the behavior of these physiological and biophysical variables (Croft et al., 2014b), as a result of varying dependency on different environmental drivers, may have large implications for the monitoring and parameterization of key terrestrial processes, including gross primary production (GPP).

Remote sensing techniques have tremendous potential to provide a cost-effective, spatially continuous means of monitoring the dynamic properties of tree biophysical variables at a range of different spatial and temporal scales. The estimation of vegetation

* Corresponding author. Tel.: +1 4169783375.
E-mail address: holly.croft@utoronto.ca (H. Croft).

http://dx.doi.org/10.1016/j.jag.2014.06.005
0303-2434/

characteristics from remotely-sensed reflectance data is often achieved through the development of statistical relationships between canopy or leaf variables and spectral vegetation indices (VI). This approach can be subject to error and uncertainty in spatially heterogeneous regions, but is less of a concern in closed broadleaf canopies, which essentially behave as a 'big leaf' (Gamon et al., 2010). In order to investigate the temporal behavior of LAI and chlorophyll over a growing season at a landscape scale, the biomass-sensitive, normalized difference vegetation index (NDVI) is used to represent LAI, and a red-edge vegetation index (Macc01) to represent leaf chlorophyll content. The widely used phenology software Timesat (Jonsson and Eklundh, 2002; Jönsson and Eklundh, 2004) is used to extract phenological metrics from the chlorophyll- and LAI-sensitive VIs, such as the start/end of growing season, in order to quantify differences in seasonal timings. The specific objectives of this study are to: (1) investigate the temporal variations of chlorophyll content and LAI across a growing season; (2) assess the impact of the selected VI on differences in retrieved key phenological metrics; (3) model spatial variations in chlorophyll content and LAI at the landscape scale.

Methods

Study site and data collection

Field sampling was conducted in 2004 in a mature sugar maple (*Acer saccharum* M.) stand located in Haliburton Forest, Ontario, Canada (45°14′16″N, 78°32′18″W). Haliburton forest falls within the Great-Lakes – St.-Lawrence region (Rowe, 1972) and is dominated by sugar maple but also contains beech (*Fagus grandifolia* Ehrh.), eastern hemlock (*Tsuga canadensis* (L.) Carr.), and yellow birch (*Betula alleghaniensis* Britt.) (Caspersen and Saprunoff, 2005). The upland hardwood forests experience an average annual precipitation of approximately 1050 mm and mean annual temperature of 5 °C (Gradowski and Thomas, 2006). The site is underlain by shallow brunisols or juvenile podzols, (pH 4.2–5.1); mainly silty sands from Precambrian Shield granite or granite-gneiss deposits (Gradowski and Thomas, 2006).

Leaves were sampled from the upper canopy of representative trees using a mobile canopy lift 8 times throughout the growing season from May 27th to September 30th (Zhang et al., 2007), within a 50 m × 30 m area. On each date, three trees were sampled, from which three branches were selected and three leaves sampled from each branch, giving a total of 27 leaf samples per sampling date. The sampled branches were tagged to ensure repeatable measurements through the growing season. Leaf samples were sealed in plastic bags and kept at a temperature of 0 °C for subsequent biochemical analysis to extract leaf chlorophyll content ($\mu g/cm^2$) (Zhang et al., 2007). Leaf area index and canopy structural parameters were measured 10 times across the growing season, along a 100 m transect. Effective LAI (*Le*) was measured by the LAI-2000 plant canopy analyser (Li-Cor, Lincoln, NE, USA), using the methods of Chen et al. (1997). The element clumping index was measured using the TRAC (Tracing Radiation and Architecture of Canopies) instrument (Chen and Cihlar, 1995).

Satellite data acquisition and processing

The MEdium Resolution Imaging Spectrometer (MERIS) on board the ENVISAT platform measures surface reflectance in fifteen spectral bands from 415 to 885 nm, with a temporal revisit time of 2–3 days. Thirty-three MERIS Reduced Resolution (RR) Level 2 (1200 m) images were used in this study, spanning the growing season from 28th March to 30th November, 2004. The L2 products contain geolocated geophysical parameters in addition to surface reflectance, including terrain height, geometric information, solar and viewing geometry, meteorological data and several flags addressing image quality (Canisius et al., 2010). MERIS L2 products were radiometrically and atmospherically corrected to account for Rayleigh scattering, ozone, water vapor absorption and aerosol content. The MERIS images were reprojected to WGS 84 and coordinate system (UTM 18) and resampled using nearest neighbor interpolation using the BEAM VISAT software application (European Space Agency). The images were also co-registered and geometrically corrected using a grid of tie points, which contained geo-location coordinates and were distributed evenly throughout the image.

Vegetation index selection

A large number of vegetation indices have been developed and tested over a range of species and physiological conditions, using empirical and simulated data (Blackburn, 2007). This study uses the Macc01 vegetation index (Maccioni et al., 2001), calculated as:

$$\text{Macc01} = \frac{\text{R780} - \text{R710}}{\text{R780} - \text{R680}} \quad (1)$$

based on the findings of a recent study (Croft et al., 2014a), which tested the relationship between 60 vegetation indices and chlorophyll content at leaf and canopy scales. Macc01 displayed a very strong relationship with chlorophyll content at the canopy scale ($R^2 = 0.93$; RMSE = 1.68 $\mu m/cm^2$) and is one of several vegetation indices based on reflectance from wavelengths along the red-edge spectral region (Dash and Curran, 2004; Gitelson and Merzlyak, 1994; Vogelmann et al., 1993; Zarco-Tejada et al., 2001). Research has shown that the red edge region is sensitive to a wider range of chlorophyll content than chlorophyll absorption bands (680 nm), which are more likely to saturate under high chlorophyll conditions (Sims and Gamon, 2002).

Whilst interactions of chlorophyll with radiation are largely limited to optical wavelengths, ranging from 400 nm to 725 nm, LAI impacts occur in the NIR, due to canopy structure and multiple scattering which is particularly important at NIR wavelengths as little radiation is absorbed (Asner, 1998). NDVI (Eq. (2)) has been extensively used to estimate LAI, along with $FAPAR_{canopy}$ and gross primary production (Potter, 1993; Running et al., 2004).

$$\text{NDVI} = \frac{\text{NIR} - \text{red}}{\text{NIR} + \text{Red}} \quad (2)$$

NDVI has a very long time record of data usage, dating from early 1980s, and is very widely used and well documented in the literature (Xiao et al., 2009). Some care has to be taken using NDVI in regions of high LAI due to saturation and reduced sensitivity. Nevertheless, Soudani et al. (2012) found a very close agreement between NDVI measured using a network of ground-based sensors and physical measurements of LAI in a number of different ecosystems, which they used to monitor temporal dynamics in phenology and canopy structure.

The relationships of NDVI and Macc01 derived from satellite reflectance data with measured LAI and leaf chlorophyll content respectively, are shown in Fig. 1. Where ground sampling dates did not exactly coincide with remotely-sensed image dates, the values of spectral indices were temporally linearly interpolated to give results for the same ground date.

Fig. 1 demonstrates that both vegetation indices show a strong relationship with their respective vegetation parameter (LAI: $R^2 = 0.67$; Chlorophyll: $R^2 = 0.97$). Despite NDVI being prone to saturation at high LAI values, Fig. 1a displays a linear relationship, with the lower LAI values corresponding to the start and end of the season clearly identifiable and the NDVI values toward the middle of the growing season relatively consistent, with little variation in LAI

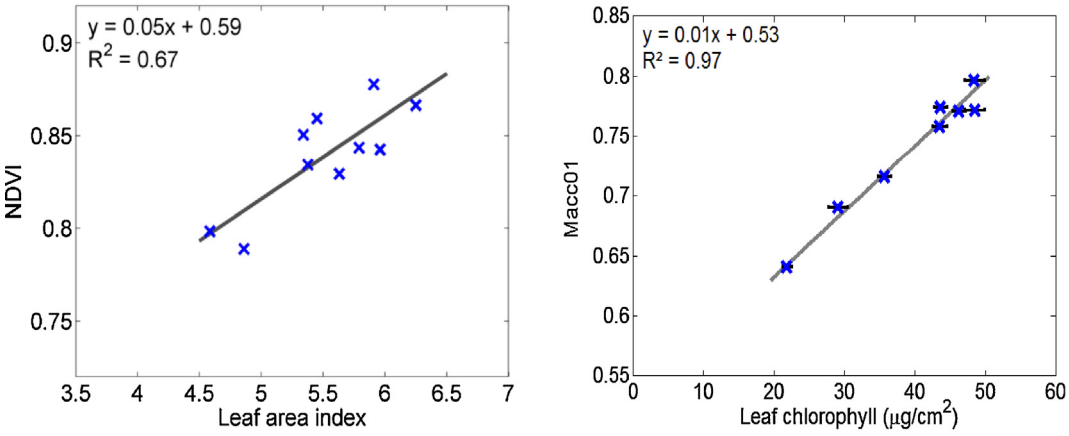

Fig. 1. The relationship between satallite-derived vegetation indices and measured ground data for (a) NDVI and LAI; (b) Macc01 and leaf chlorophyll content (error bars represent the standard error).

values. Fig. 1 supports the use of both indices as a proxy for the respective LAI or leaf chlorophyll content in this study.

Comparison between MERIS reduced resolution and full resolution data

It was necessary to use MERIS RR images (1200 m) in this study rather than (FR) full resolution (300 m) data due to the partial availability of FR images over North America before April 2008, as a result of the limited capacity for systematic archiving of MERIS FR imagery before this time. The reduced number of FR images archived during 2004 failed to capture important phenological stages of the growing season and resulted in coarser time intervals. Nevertheless, the available FR MERIS images over the growing season were downloaded and the results compared to the RR data (Fig. 2) to investigate possible effects of spatial heterogeneity on results as a result of the differing spatial resolutions of the products.

The very close agreement of data derived from MERIS RR and FR products shown in Fig. 2 is due to the homogeneity of the broadleaf forest site, and justifies the use of RR data in order to obtain the benefits of the finer temporal resolution and greater number of images available for analysis.

Deriving phenological metrics

The VI time-series data was processed using TIMESAT version 3.1.1 software (Jönsson and Eklundh, 2002, 2004), which was developed for fitting mathematical functions to satellite time-series data to extract seasonal parameters. TIMESAT has been used in a number of ecological applications, including mapping environmental and phenological changes (Olsson et al., 2005), the development of carbon models using satellite data (Olofsson et al., 2008) and forest disturbances detection (Eklundh et al., 2009). VI time series data can often contains spurious variation caused by atmospheric variability and bidirectional reflectance distribution function (BRDF) effects which affect the monitoring of terrestrial ecosystems (Chen et al., 2004). The logistic curve function has been widely used to smooth the VI time series and extract key phenological metrics (Fisher et al., 2006; Richardson et al., 2009a; Zhang et al., 2003). We used a double logistic curve function (Eq. (3)), which Hird and McDermid (2009) found maintained NDVI signal integrity (Jönsson et al., 2010).

$$g(t; x1, \ldots, x4) = \frac{1}{1 + \exp(x1 - t/x2)} - \frac{1}{1 + \exp(x3 - t/x4)} \quad (3)$$

where t is time in days, and $x1$ and $x3$ determine the position of the left and right inflection point respectively, representing canopy development and senescence, and $x2$ and $x4$ give the respective rate of change. Key phenological metrics were extracted from the fitted curve function, including start of season (SOS), end of season (EOS), growing season duration (EOS-SOS), amplitude and slope of right and left curve. The SOS and EOS were estimated as 30% of the rising and falling limb, respectively. The amplitude is the difference between the maximum value and the base level. As Timesat only works on multiple years, the growing season was duplicated to make an artificial time-series spanning three years and extracted

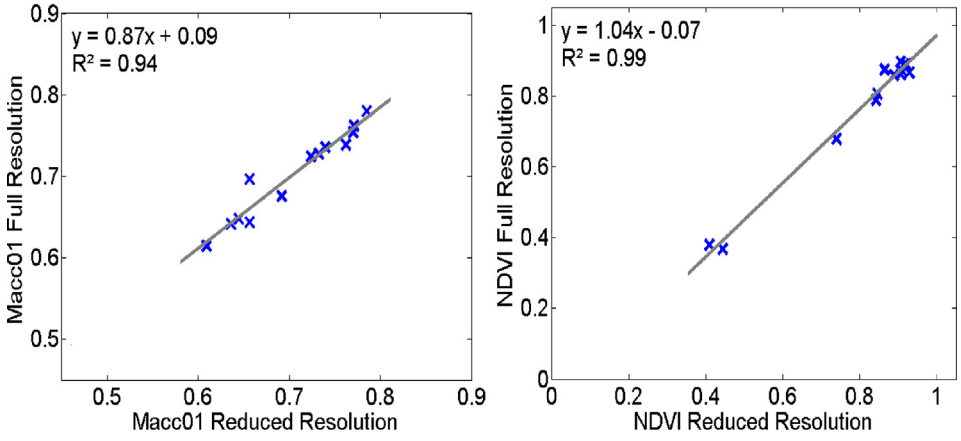

Fig. 2. Comparison of MERIS reduced resolution and full resolution data, for (a) Macc01 and (b) NDVI.

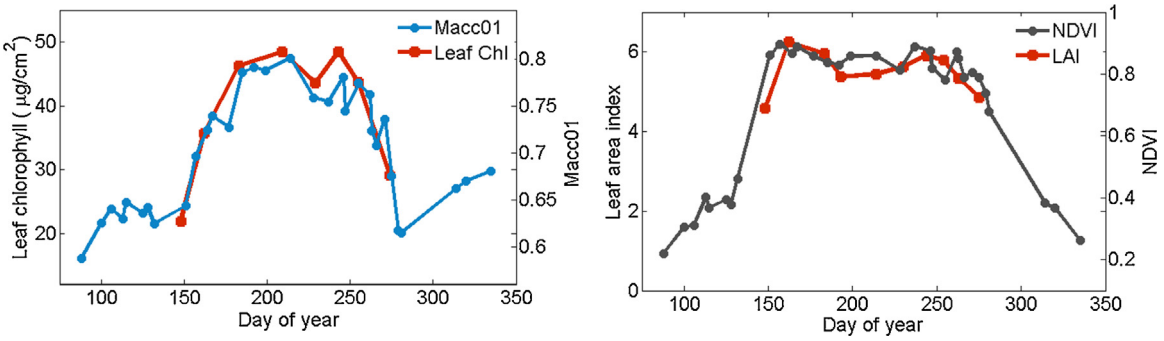

Fig. 3. Ground measurements and satellite-derived VI values for (a) Chlorophyll and (b) LAI across a growing season.

metrics from the middle season of the time-series (Eklundh and Jönsson, 2010). Along with many smoothing functions, Timesat only accepts data sampled at uniform intervals, consequently the VI time series was resampled to regular 5-day intervals in order to fit the logistic curve. Only very negligible differences were present between the original and resampled time series. All figures in subsequent sections show the data as collected at original acquisition times with the exception of the logistic curve function.

Results

Variations in chlorophyll and LAI across a growing season

Prior to spatiotemporal analysis across broader spatial extents, the correlation between ground measurements of leaf chlorophyll and LAI with satellite derived VIs across a growing season are first investigated. The chlorophyll index (Macc01) was found to be a top performing chlorophyll index at the canopy level (Croft et al., 2014a). The NDVI index used as a proxy for LAI and has been widely used to delineate plant growing season (Jenkins et al., 2002; Xiao et al., 2009). Fig. 3 shows the satellite-derived VIs representing Chlorophyll (Macc01) and LAI (NDVI) for one pixel corresponding to ground measurement locations and measured leaf chlorophyll content and LAI.

Both the Macc01 and NDVI index show very close relationships to changes over time in chlorophyll and LAI, respectively. Ground measurements of chlorophyll ($\mu g/cm^2$) and LAI exhibit a strong temporal consistency with Macc01 and NDVI at the start and end of the growing season. After the initial 'greening up' stage at the start of the growing season, the NDVI and LAI data both show relatively stable values with time compared to the chlorophyll and Macc01 values. This strong correlation between the VIs and respective ground measurements demonstrates the suitability for each VI to act as a proxy for its respective ecological variable. To investigate the temporal nature of changes in chlorophyll and LAI across a growing season, the two VIs are shown together in Fig. 4.

Clear differences can be seen in the temporal profile of chlorophyll and LAI across the season, particularly in the early stages, following bud burst (Fig. 4). LAI increases begin earlier and are more rapid than changes in chlorophyll content, with a start date of approximately day of year (DOY) 132 and reaching maximum values by DOY 151. By contrast chlorophyll remains stable until approximately DOY151, and then begins to increase more gradually until DOY 185. Fig. 4 demonstrates that, whilst the leaves are out, the leaf chlorophyll content remains low for a period after this event, which may impact photosynthetic rates. It is possible that the sudden increase in NDVI values at DOY 132 is responding to understory greening prior to the main canopy bud burst. However, Jenkins et al. (2002) used a NDVI threshold of 0.45 to define the start of the plant growing season for forests in the eastern USA, which corresponds to the results seen at a start DOY of 132 in Fig. 4.

In order to quantify variations in the temporal profile between chlorophyll content and LAI, logistic curve functions were fitted to the VIs using Timesat software (Jönsson and Eklundh, 2002, 2004), to derive key phenological metrics. The logistic curve was fitted to temporally resampled data at 5-day intervals and is shown with the VI at the original acquisition time intervals (Fig. 5).

The fitted curve functions in Fig. 5 show clear temporal differences, with the chlorophyll growing season appearing to be much shorter in duration, both starting later and ending earlier. Whilst the chlorophyll curve is relatively symmetrical, LAI shows a sharp increase at the start of the season, following bud burst and a more gradual decline at the end of the season, with senescence and leaf fall, leading to a more asymmetrical temporal profile. Phenological metrics were extracted from the logistic models to quantify important phenological stages and compare with the two VIs, including start and end of season dates and season length (Table 1).

The apparent temporal differences in chlorophyll and LAI indices seen in Fig. 5 are confirmed by the derived phenological metrics (Table 1). The LAI season duration is 57 days longer than the chlorophyll season, and begins 27 days earlier at DOY 130. Whilst the SOS, EOS and season duration dates are very different, the peak time for both VIs is only 4 days apart (DOY 221 and 217 for Macc01 and NDVI, respectively).

Spatial heterogeneity in temporal chlorophyll and LAI dynamics

Several studies have found that vegetation phenology is not uniform across space and displays complex spatial patterns at a number of different spatial scales (Richardson et al., 2009a). Fig. 6 shows how chlorophyll content, derived from Macc01, varies spatially on key dates across a growing season across a 72×72 km spatial extent, centralized on the ground field site.

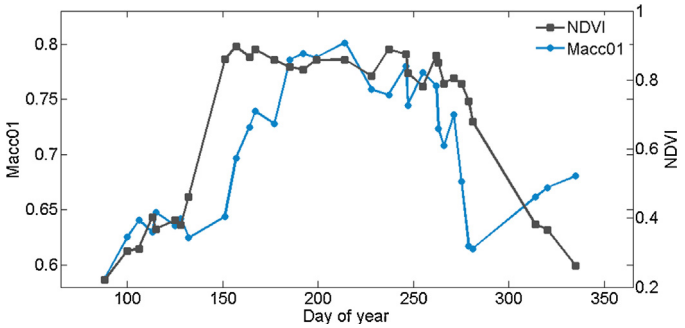

Fig. 4. Temporal variations in Chlorophyll (Macc01) and LAI (NDVI) across a growing season.

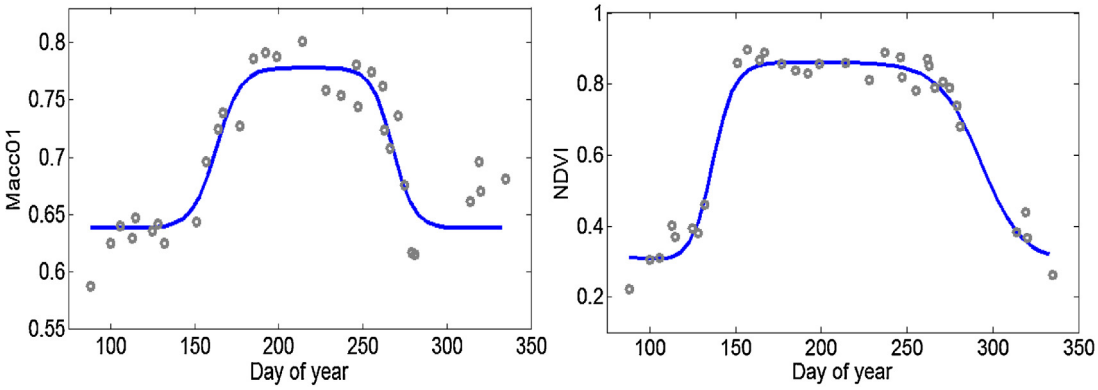

Fig. 5. Differences in chlorophyll content (represented by Macc01) and LAI (represented by NDVI) across a growing season.

Table 1
Phenological metrics for chlorophyll content (Macc01) and LAI (NDVI).

	Start	End	Length	Base value	Peak DOY	Peak value	Amplitude	Left derivative	Right derivative
Macc01	157	278	121	0.63	221	0.78	0.15	0.017	0.024
NDVI	130	308	178	0.28	217	0.86	0.58	0.063	0.050

Even within a 72 × 72 km region, Fig. 6 shows that chlorophyll content varies considerably across space throughout the growing season. Notably, whilst spatial differences in chlorophyll are evident, they appear to be relatively stable with time, with the localized higher Macc01 values at DOY 199 (circa 0.79), also persisting later in the growing season at DOY 262. Broadly the same areas of lower chlorophyll contents are also present from DOY 157 to DOY 214, after which they become integrated into coarser patches of more spatially continuous chlorophyll content. There is a slight decrease in chlorophyll from DOY 132 to DOY 151,

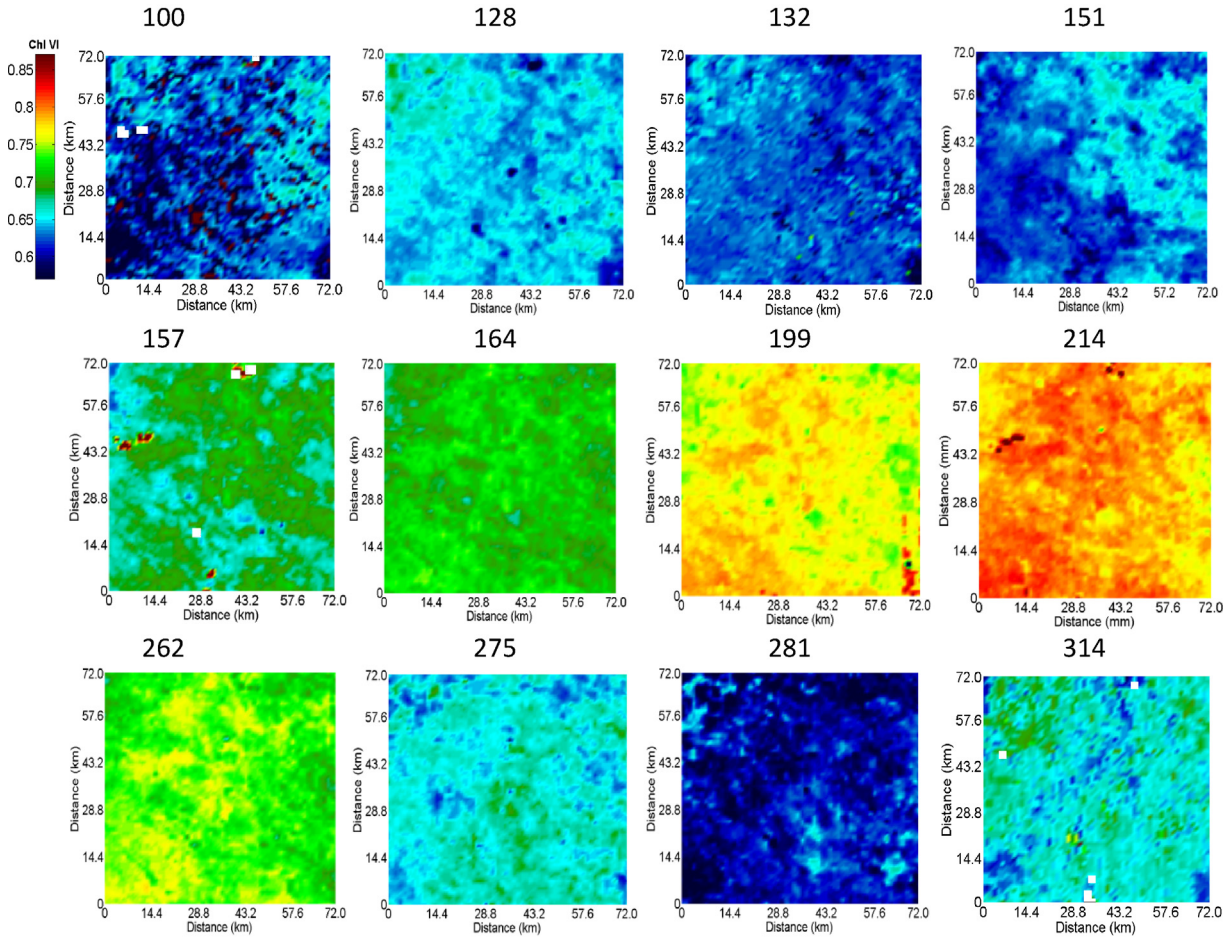

Fig. 6. Spatial variability of chlorophyll content (Macc01) across a growing season.

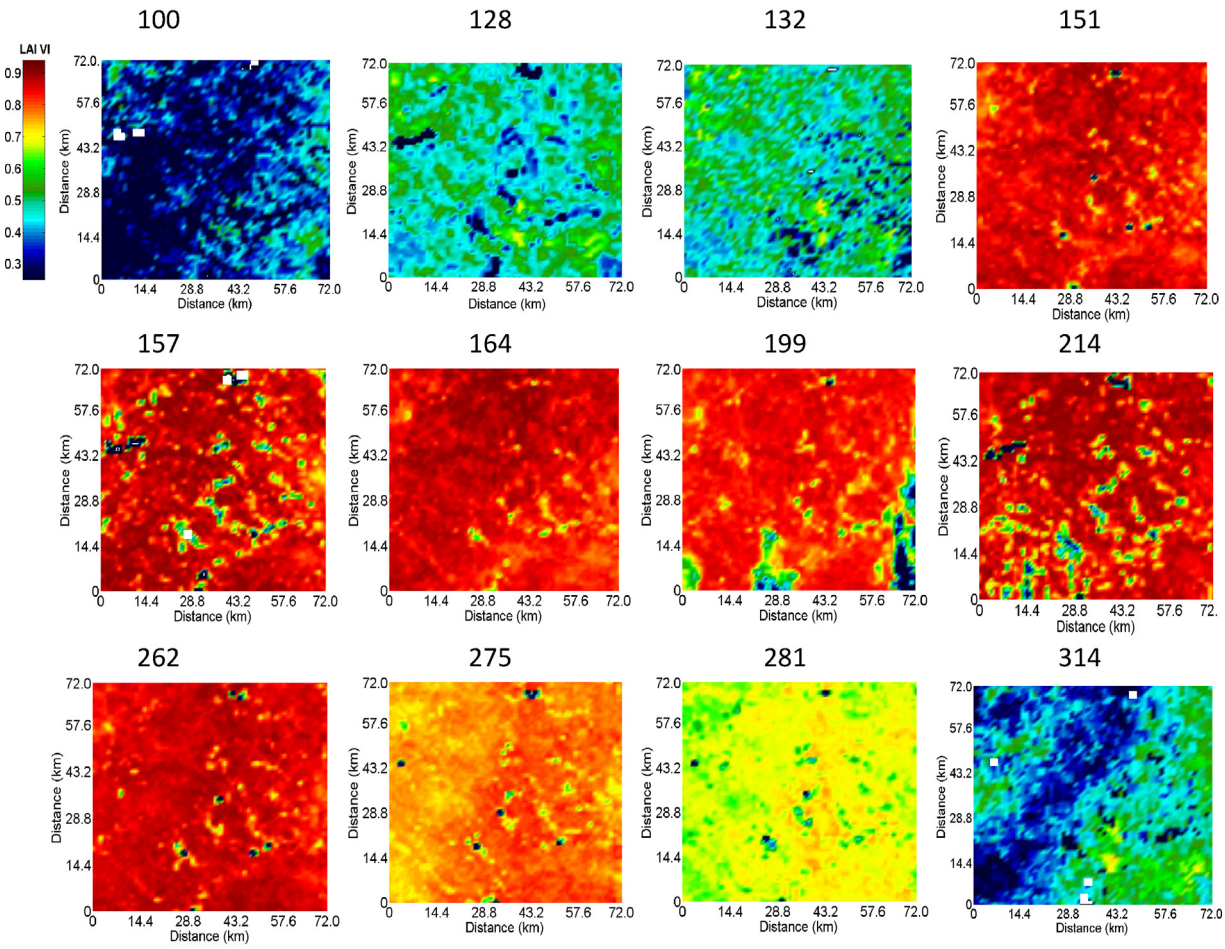

Fig. 7. Spatial variability of LAI (NDVI) across a growing season.

relative to the DOY 128 results. This apparent decrease could be a false signal at DOY 128, as a result of understory growth or canopy bud burst, and temporally corresponds to the increase in NDVI values relating to LAI. The spatial variability visible in Fig. 6 may be due to differences in forest species or differences in chlorophyll content within species.

The spatial distribution and temporal dynamics of LAI (NDVI) shown in Fig. 7 reveal contrasting results to those of leaf chlorophyll content. The spatial representation of the LAI time-series confirm the findings in Fig. 5; illustrating an abrupt change in LAI across space for the start of the growing season and a slower change at the end of the growing season, with relatively consistent overall values for the remainder (approximately NDVI = 0.9).

In contrast to chlorophyll content, the spatial scales of LAI variability appears to change with time, with spatial variations in NDVI in the middle of the growing season being more localized, with smaller patch sizes and greater extreme differences in value. At the start and end of the season, coarser scales of spatial variability were also present. This is in contrast to chlorophyll distribution which displayed larger, more coherent structures, the length-scale of which did not generally appear to change with time.

Spatial variability in the start and end of the growing season

The modeled phenological metrics for the start and end of the growing season for LAI and leaf chlorophyll are shown spatially in Fig. 8, along with the difference in days between the chlorophyll and LAI SOS and EOS (Fig. 8c and f). A double logistic model was used; following the methods used previsouly, with SOS and EOS metrics extracted at 30% of the rising and falling limb, respectively.

The modeled SOS and EOS days shown across a 72 × 72 km spatial extent confirm the results shown in Table 1 for one pixel, with Macc01 SOS occuring around DOY 155–160, and NDVI SOS predominately occurring between 132 and 138. The EOS occured between DOY 267–275 for Macc01 and DOY 290–310 for NDVI. Whilst there is spatial variation across the landscape in phenological metrics for each VI, the temporal range is relatively small, particularly at the SOS where most variation for both indices was within ±5 days. The spatial variation in leaf chlorophyll (Macc01) SOS onset was comprised of coarser-scale patches across the lansdcape, in comparison to NDVI, where more fine-scale dissimilarity was visible. Fig. 8c and f also show the large discrepencies between leaf chlorophyll and LAI SOS and EOS that exist spatially, with chlorophyll SOS occuring approximately +20–35 days after LAI SOS, and chlorophyll EOS occuting approximately −20–30 before LAI EOS.

Discussion

Spatio-temporal variations in LAI and chlorophyll content

The main phenological phases can be seen in the growth curve of both chlorophyll and LAI VIs (Figs. 3 and 4), including a first phase of growth related to budburst, leaf development and maturation in spring and senescence and leaf fall in autumn (Soudani et al., 2012). However, results indicate the timing of changes in chlorophyll and LAI (as represented by Macc01 and NDVI) across a season are very different. LAI increased earlier in the season and more rapidly than

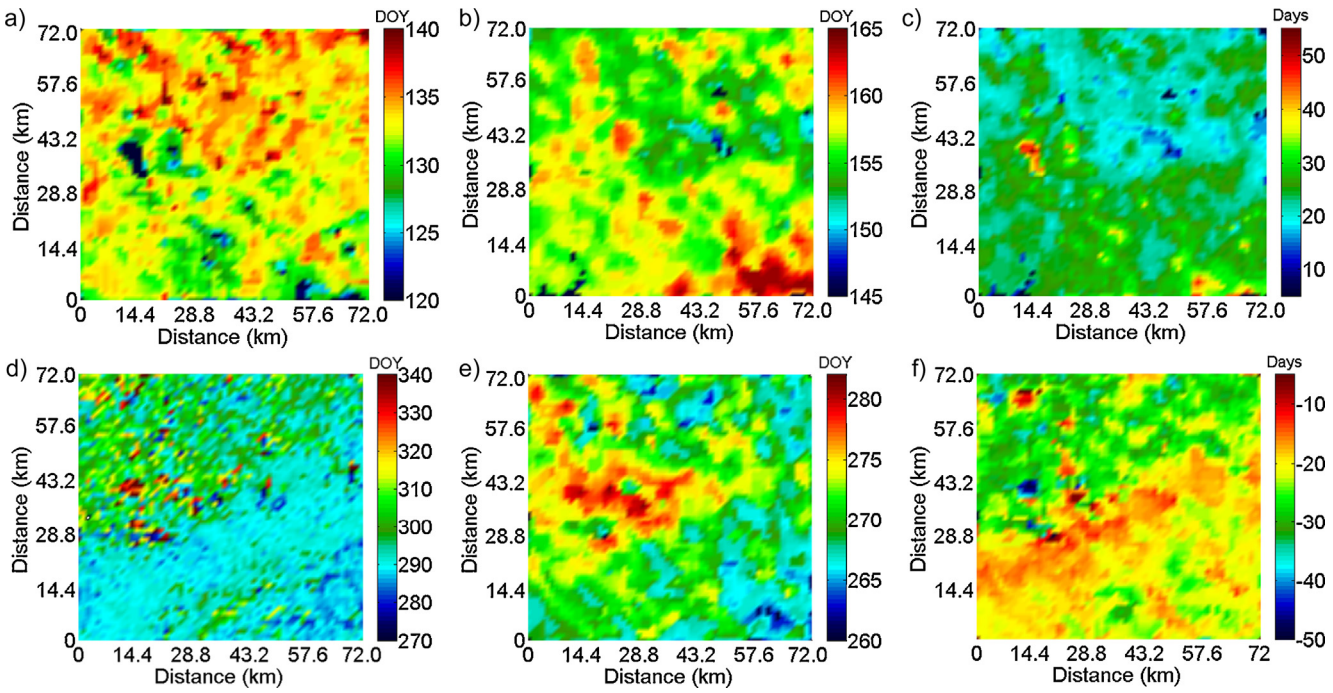

Fig. 8. The start of the growing season for (a) NDVI, (b) Macc01, by day of year, (c) the difference in days between Macc01 and NDVI SOS, and the end of the growing season for (d) NDVI, (e) Macc01, by day of year, (f) the difference in days between Macc01 and NDVI EOS.

chlorophyll content, which took a longer period of time to reach maximum values (Fig. 4). Extracted phenological metrics indicated that the start of season dates varied by 27 days (DOY 130 and 157 for LAI and chlorophyll, respectively). This finding confirmed previous research by Kodani et al. (2002) on a Japanese beech (*Fagus crenata*) stand, who found that start of season changes in LAI preceded those for chlorophyll content. The results follow physiological development of the canopy, where in spring, leaves are first formed and chlorophyll accumulated, and in the autumn the chlorophyll is decomposed and nitrogen withdrawn before leaf fall (Kodani et al., 2002). This pattern was also shown by Nagai et al. (2011) who studied *Betula ermanii*, *Quercus crispula* and *Acer rufinerve*, finding that in all cases LAI was characterized by a sharp increase on bud expansion, with chlorophyll measured by SPAD displaying a more gradual increase, taking longer to reach maximum values. This relationship varied between species, with the chlorophyll in *A. rufinerve* trees showing the greater lag and slowest development. Furthermore, the decline in values at the end of the season occurs sooner for the chlorophyll VI, indicating the breakdown of chlorophyll and cessation of photosynthetic processes can be captured prior to leaf fall. The nature of the relationship between chlorophyll and LAI development during leaf expansion and senescence for different species and under different environmental conditions requires further research. The difference in growing season metrics indicates that the choice of spectral index is crucial to obtaining accurate information on the processes of interest, e.g. in relation to canopy structure or to leaf function. The phenological metrics for both LAI and chlorophyll also displayed distinct spatial variations at the landscape scale (Fig. 8), which may be related to differences in drainage patterns, water availability and local topography.

VI derived LAI or chlorophyll content for estimating GPP

This research has shown clear differences in the spatial and temporal dynamics of chlorophyll and LAI, retrieved from satellite-derived VIs. The findings have potentially far reaching implications in the estimation, monitoring and parameterization of key terrestrial processes, including gross primary production (GPP). The fraction of photosysnthetically active radiation (400–700 nm; FAPAR) is an important variable in the estimation of GPP, and is commonly used in satellite-based Production Efficiency Models (Ruimy et al., 1996; Running et al., 2004). $FAPAR_{canopy}$ is usually estimated as a function of NDVI represented by the empirical relationship NDVI–LAI–$FPAR_{canopy}$ (Zhang et al., 2005). However, as chlorophyll is the 'photosynthetic apparatus' of the plant (Peng et al., 2013), only the PAR absorbed by chlorophyll is used for photosynthesis (Zhang et al., 2009). Research by Zhang et al. (2005) found differences between $FAPAR_{canopy}$ and $FAPAR_{chl}$ and suggested that using $FAPAR_{chl}$ to estimate GPP in biogeochemical models would be better representative of plant photosynthesis processes. Studies have also demonstrated that leaf chlorophyll content was well correlated with temporal changes in light use efficiency (LUE) (Peng et al., 2011; Wu et al., 2009). In crop studies, researchers have also found a close relationship between canopy chlorophyll content and GPP, where total chlorophyll content appeared to be a good proxy of maize GPP (Gitelson et al., 2003, 2006; Peng et al., 2011).

Conclusion

This research investigated differences in temporal and spatial variation of chlorophyll content and LAI at the landscape scale. It sought to begin to address the need for better understanding of the relationships between phenology and ecological functionality called for by Liang and Schwartz (2009) and demonstrated that phenology, both in terms the timing of bud burst and leaf development, vary spatially over a landscape. In addition to differing spatial distributions, chlorophyll and LAI VIs also displayed extremely different temporal profiles, with the duration of the LAI season was found to be 178 days in length, compared to chlorophyll, which was 121 days. The LAI season also preceded the start of the chlorophyll season by 27 days (DOY 130 and 157, respectively). This study highlights the differences that exist between chlorophyll (Macc01)

and LAI (NDVI) for a broadleaf forest over time and space, indicating that there is an important implication for biogeochemical models that fail to account for the delay in chlorophyll production post leaf expansion. The potential differences that exist between $FAPAR_{canopy}$ and $FAPAR_{chl}$ over time for a deciduous canopy could lead to overestimations in light absorption and GPP by models that use $FAPAR_{canopy}$, particularly during the early stages of the growing season.

References

Asner, G.P., 1998. Biophysical and biochemical sources of variability in canopy reflectance. Remote Sens. Environ. 64, 234–253.

Blackburn, G.A., 2007. Hyperspectral remote sensing of plant pigments. J. Exp. Bot. 58, 855–867.

Boegh, E., Soegaard, H., Broge, N., Hasager, C.B., Jensen, N.O., Schelde, K., Thomsen, A., 2002. Airborne multispectral data for quantifying leaf area index, nitrogen concentration, and photosynthetic efficiency in agriculture. Remote Sens. Environ. 81, 179–193.

Canisius, F., Fernandes, R., Chen, J., 2010. Comparison and evaluation of Medium Resolution Imaging Spectrometer leaf area index products across a range of land use. Remote Sens. Environ. 114, 950–960.

Caspersen, J.P., Saprunoff, M., 2005. Seedling recruitment in a northern temperate forest: the relative importance of supply and establishment limitation. Can. J. Forest Res. 35, 978–989.

Carter, G.A., Knapp, A.K., 2001. Leaf optical properties in higher plants: linking spectral characteristics to stress and chlorophyll concentration. Am. J. Bot. 88, 677–684.

Chen, J.M., Black, T.A., 1992. Defining leaf area index for non-flat leaves. Plant Cell Environ. 15, 421–429.

Chen, J.M., Cihlar, J., 1995. Plant canopy gap-size analysis theory for improving optical measurements of leaf-area index. Appl. Opt. 34, 6211–6222.

Chen, J.M., Plummer, P.S., Rich, M., Gower, S.T., Norman, J.M., 1997. Leaf area index measurements. J. Geophys. Res. 102, 29–429.

Chen, J., Jönsson, P., Tamura, M., Gu, Z., Matsushita, B., Eklundh, L., 2004. A simple method for reconstructing a high-quality NDVI time-series data set based on the Savitzky–Golay filter. Remote Sens. Environ. 91, 332–344.

Churkina, G., Schimel, D., Braswell, B.H., Xiao, X., 2005. Spatial analysis of growing season length control over net ecosystem exchange. Global Change Biol. 11, 1777–1787.

Croft, H., Chen, J.M., Zhang, Y., Simic, A., 2013. Modelling leaf chlorophyll content in broadleaf and needle leaf canopies from ground, CASI, Landsat TM 5 and MERIS reflectance data. Remote Sens. Environ. 133, 128–140.

Croft, H., Chen, J.M., Zhang, Y., 2014a. The applicability of empirical vegetation indices for determining leaf chlorophyll content over different leaf and canopy structures. Ecol. Complex 17, 119–130.

Croft, H., Chen, J.M., Noland, T., 2014b. Stand age effects on Boreal forest physiology using a long time-series of satellite data. For. Ecol. Manage. 328, 202–208.

Dash, J., Curran, P.J., 2004. The MERIS terrestrial chlorophyll index. Int. J. Remote Sens. 25, 5403–5413.

Demarez, V., Gastellu-Etchegorry, J.P., Mougin, E., Marty, G., Proisy, C., Dufrêne, E., Dantec, V.L., 1999. Seasonal variation of leaf chlorophyll content of a temperate forest. Inversion of the PROSPECT model. Int. J. Remote Sens. 20, 879–894.

Eklundh, L., Johansson, T., Solberg, S., 2009. Mapping insect defoliation in Scots pine with MODIS time-series data. Remote Sens. Environ. 113, 1566–1573.

Eklundh, L., Jönsson, P., 2010. Timesat 3.0 Software Manual.

Fisher, J.I., Mustard, J.F., Vadeboncoeur, M.A., 2006. Green leaf phenology at Landsat resolution: scaling from the field to the satellite. Remote Sens. Environ. 100, 265–279.

Gamon, J.A., Coburn, C., Flanagan, L.B., Huemmrich, K.F., Kiddle, C., Sanchez-Azofeifa, G.A., Thayer, D.R., Vescovo, L., Gianelle, D., Sims, D.A., 2010. SpecNet revisited: bridging flux and remote sensing communities. Can. J. Remote Sens. 36, 376–390.

Gitelson, A., Merzlyak, M.N., 1994. Quantitative estimation of chlorophyll-a using reflectance spectra: experiments with autumn chestnut and maple leaves. J. Photochem. Photobiol. B: Biol. 22, 247–252.

Gitelson, A.A., Verma, S.B., Vina, A., Rundquist, D.C., Keydan, G., Leavitt, B., Arkebauer, T.J., Burba, G.G., Suyker, A.E., 2003. Novel technique for remote estimation of CO_2 flux in maize. Geophys. Res. Lett. 30, 29–31.

Gitelson, A.A., Viña, A., Verma, S.B., Rundquist, D.C., Arkebauer, T.J., Keydan, G., Leavitt, B., Ciganda, V., Burba, G.G., Suyker, A.E., 2006. Relationship between gross primary production and chlorophyll content in crops: implications for the synoptic monitoring of vegetation productivity. J. Geophys. Res. D: Atmos. 111, D08S11.

Gradowski, T., Thomas, S.C., 2006. Phosphorus limitation of sugar maple growth in central Ontario. For. Ecol. Manage. 226, 104–109.

Hird, J.N., McDermid, G.J., 2009. Noise reduction of NDVI time series: an empirical comparison of selected techniques. Remote Sens. Environ. 113, 248–258.

Houborg, R., Boegh, E., 2008. Mapping leaf chlorophyll and leaf area index using inverse and forward canopy reflectance modeling and SPOT reflectance data. Remote Sens. Environ. 112, 186–202.

Jenkins, J.P., Braswell, B.H., Frolking, S.E., Aber, J.D., 2002. Detecting and predicting spatial and interannual patterns of temperate forest springtime phenology in the eastern US. Geophys. Res. Lett. 29, 2201.

Jonsson, P., Eklundh, L., 2002. Seasonality extraction by function fitting to time-series of satellite sensor data. IEEE Trans. Geosci. Remote Sens. 40, 1824–1832.

Jönsson, P., Eklundh, L., 2002. Seasonality extraction by function fitting to time-series of satellite sensor data. IEEE Trans. Geosci. Remote Sens. 40, 1824–1832.

Jönsson, P., Eklundh, L., 2004. TIMESAT – a program for analyzing time-series of satellite sensor data. Comput. Geosci. 30, 833–845.

Jönsson, A.M., Eklundh, L., Hellström, M., Bärring, L., Jönsson, P., 2010. Annual changes in MODIS vegetation indices of Swedish coniferous forests in relation to snow dynamics and tree phenology. Remote Sens. Environ. 114, 2719–2730.

Kodani, E., Awaya, Y., Tanaka, K., Matsumura, N., 2002. Seasonal patterns of canopy structure, biochemistry and spectral reflectance in a broad-leaved deciduous *Fagus crenata* canopy. For. Ecol. Manage. 167, 233–249.

Liang, L., Schwartz, M.D., 2009. Landscape phenology: an integrative approach to seasonal vegetation dynamics. Landscape Ecol. 24 (4), 465–472.

Maccioni, A., Agati, G., Mazzinghi, P., 2001. New vegetation indices for remote measurement of chlorophylls based on leaf directional reflectance spectra. J. Photochem. Photobiol. B: Biol. 61, 52–61.

Morin, X., Lechowicz, M.J., Augspurger, C., O'Keefe, J., Viner, D., Chuine, I., 2009. Leaf phenology in 22 North American tree species during the 21st century. Global Change Biol. 15, 961–975.

Morisette, J.T., Richardson, A.D., Knapp, A.K., Fisher, J.I., Graham, E.A., Abatzoglou, J., Wilson, B.E., Breshears, D.D., Henebry, G.M., Hanes, J.M., Liang, L., 2009. Tracking the rhythm of the seasons in the face of global change: phenological research in the 21st century. Front. Ecol. Environ. 7, 253–260.

Nagai, S., Maeda, T., Gamo, M., Muraoka, H., Suzuki, R., Nasahara, K.N., 2011. Using digital camera images to detect canopy condition of deciduous broad-leaved trees. Plant Ecol. Divers. 4, 79–89.

Olofsson, P., Lagergren, F., Lindroth, A., Lindström, J., Klemedtsson, L., Kutsch, W., Eklundh, L., 2008. Towards operational remote sensing of forest carbon balance across Northern Europe. Biogeosciences 5, 817–832.

Olsson, L., Eklundh, L., Ardö, J., 2005. A recent greening of the Sahel – trends, patterns and potential causes. J. Arid Environ. 63, 556–566.

Peng, Y., Gitelson, A.A., Keydan, G., Rundquist, D.C., Moses, W., 2011. Remote estimation of gross primary production in maize and support for a new paradigm based on total crop chlorophyll content. Remote Sens. Environ. 115, 978–989.

Peng, Y., Gitelson, A.A., Sakamoto, T., 2013. Remote estimation of gross primary productivity in crops using MODIS 250 m data. Remote Sens. Environ. 128, 186–196.

Pfeifer, M., Disney, M., Quaife, T., Marchant, R., 2012. Terrestrial ecosystems from space: a review of earth observation products for macroecology applications. Global Ecol. Biogeogr. 21, 603–624.

Potter, C.S., 1993. Terrestrial ecosystem production: a process model based on global satellite and surface data. Global Biogeochem. Cycles 7, 811–841.

Richardson, A.D., Bailey, A.S., Denny, E.G., Martin, C.W., O'Keefe, J., 2006. Phenology of a northern hardwood forest canopy. Global Change Biol. 12, 1174–1188.

Richardson, A.D., Braswell, B.H., Hollinger, D.Y., Jenkins, J.P., Ollinger, S.V., 2009a. Near-surface remote sensing of spatial and temporal variation in canopy phenology. Ecol. Appl. 19, 1417–1428.

Richardson, A.D., Hollinger, D.Y., Dail, D.B., Lee, J.T., Munger, J.W., O'Keefe, J., 2009b. Influence of spring phenology on seasonal and annual carbon balance in two contrasting New England forests. Tree Physiol. 29, 321–331.

Rowe, J.S., 1972. Forest regions of Canada. Information Canada.

Ruimy, A., Dedieu, G., Saugier, B., 1996. TURC: a diagnostic model of continental gross primary productivity and net primary productivity. Global Biogeochem. Cycles 10, 269–285.

Running, S.W., Nemani, R.R., Heinsch, F.A., Zhao, M., Reeves, M., Hashimoto, H., 2004. A continuous satellite-derived measure of global terrestrial primary production. Bioscience 54, 547–560.

Sims, D.A., Gamon, J.A., 2002. Relationships between leaf pigment content and spectral reflectance across a wide range of species, leaf structures and developmental stages. Remote Sens. Environ. 81, 337–354.

Soudani, K., Hmimina, G., Delpierre, N., Pontailler, J.Y., Aubinet, M., Bonal, D., Caquet, B., de Grandcourt, A., Burban, B., Flechard, C., 2012. Ground-based Network of NDVI measurements for tracking temporal dynamics of canopy structure and vegetation phenology in different biomes. Remote Sens. Environ. 123, 234–245.

Vogelmann, J.E., Rock, B.N., Moss, D.M., 1993. Red edge spectral measurements from sugar maple leaves. Int. J. Remote Sens. 14, 1563–1575.

Wu, C., Niu, Z., Tang, Q., Huang, W., Rivard, B., Feng, J., 2009. Remote estimation of gross primary production in wheat using chlorophyll-related vegetation indices. Agric. For. Meteorol. 149, 1015–1021.

Xiao, X., Zhang, J., Yan, H., Wu, W., Biradar, C., 2009. Land surface phenology: convergence of satellite and CO_2 eddy flux observations. In: Noormets, A. (Ed.), Phenology of ecosystem processes. Springer, New York, NY, pp. 247–270.

Zarco-Tejada, P.J., Miller, J.R., Noland, T.L., Mohammed, G.H., Sampson, P.H., 2001. Scaling-up and model inversion methods with narrowband optical indices for chlorophyll content estimation in closed forest canopies with hyperspectral data. IEEE Trans. Geosci. Remote Sens. 39, 1491–1507.

Zhang, X., Friedl, M.A., Schaaf, C.B., Strahler, A.H., Hodges, J.C.F., Gao, F., Reed, B.C., Huete, A., 2003. Monitoring vegetation phenology using MODIS. Remote Sens. Environ. 84, 471–475.

Zhang, Q., Xiao, X., Braswell, B., Linder, E., Baret, F., Moore Iii, B., 2005. Estimating light absorption by chlorophyll, leaf and canopy in a deciduous broadleaf forest using MODIS data and a radiative transfer model. Remote Sens. Environ. 99, 357–371.

Zhang, Q., Xiao, X., Braswell, B., Linder, E., Ollinger, S., Smith, M.L., Jenkins, J.P., Baret, F., Richardson, A.D., Moore, B., 2006. Characterization of seasonal variation of forest canopy in a temperate deciduous broadleaf forest, using daily MODIS data. Remote Sens. Environ. 105, 189–203.

Zhang, Y., Chen, J.M., Thomas, S.C., 2007. Retrieving seasonal variation in chlorophyll content of overstory and understory sugar maple leaves from leaf-level hyperspectral data. Can. J. Remote Sens. 33, 406–415.

Zhang, Q., Middleton, E.M., Margolis, H.A., Drolet, G.G., Barr, A.A., Black, T.A., 2009. Can a satellite-derived estimate of the fraction of PAR absorbed by chlorophyll ($FAPAR_{chl}$) improve predictions of light-use efficiency and ecosystem photosynthesis for a boreal aspen forest? Remote Sens. Environ. 113, 880–888.